Structure of the Spin-Glass State of $La_{2-x}Sr_xCuO_4$: The Spiral Theory

Andreas Lüscher,[1] Alexander I. Milstein,[2] and Oleg P. Sushkov[1]
[1]*School of Physics, University of New South Wales, Sydney 2052, Australia*
[2]*Budker Institute of Nuclear Physics, 630090 Novosibirsk, Russia*
(Received 29 June 2006; published 16 January 2007)

Starting from the t-J model, we derive the effective field theory describing the spin dynamics in insulating $La_{2-x}Sr_xCuO_4$, $x \lesssim 0.055$, at low temperature. The theory results in a disordered spiral ground state, in which the staggered component of the copper spins is confined in a plane determined by the spin anisotropies. The static spin structure factor obtained in our calculations is in perfect agreement with neutron scattering data over the whole range of doping in both, the Néel and the spin-glass phase. We show that topological defects (spin vortex-antivortex pairs) are an intrinsic property of the disordered spiral ground state.

DOI: 10.1103/PhysRevLett.98.037001 PACS numbers: 74.72.Dn, 75.10.Jm, 75.30.Fv, 75.50.Ee

Over the past two decades, much progress has been made towards a better understanding of the magnetic properties of $La_{2-x}Sr_xCuO_4$ (LSCO), the prototypical cuprate superconductor. The phase diagram of LSCO shows that the magnetic state changes tremendously with Sr doping. The three-dimensional antiferromagnetic Néel order identified [1] below 325 K in the parent compound disappears at doping $x \approx 0.02$ and gives way to the so-called spin-glass phase which extends up to $x \approx 0.055$. In the Néel and the spin-glass phase, the system essentially behaves as an Anderson insulator and exhibits only hopping conductivity. Superconductivity then sets in for doping $x > 0.055$ [2]. Despite intense theoretical research, the magnetic structure of the weakly doped region remained unexplained. In that respect, the most intriguing property of LSCO is the static incommensurate magnetic ordering observed at low temperature in elastic neutron scattering experiments. This ordering manifests itself as a scattering peak shifted with respect to the antiferromagnetic position. Very importantly, the incommensurate ordering is a generic feature of LSCO. According to experiments in the Néel phase, the incommensurability is almost doping independent and directed along the orthorhombic b axis [3]. In the spin-glass phase, the shift is also directed along the b axis, but scales linearly with doping [4–6]. Finally, in the underdoped superconducting region ($0.055 \lesssim x \lesssim 0.12$), the shift still scales linearly with doping, but it is directed along the crystal axes of the tetragonal lattice [7].

These observations caused a renewal of theoretical interest in the idea of spin spirals in cuprates, both from the phenomenological [8–11] and the microscopic [12–14] point of view. In relation to the t-J model, this idea was first formulated by Shraiman and Siggia [15], who pointed out that for an appreciable superexchange, it is energetically favorable to allow the collinear Néel state to relax and form a spiral, in which holes can propagate more easily. In this Letter, we formulate the effective field theory that describes the spin-glass phase of LSCO at low temperature. We study the ground state, calculate the spin structure factor, and analyze the nature of the phase transition from the Néel to the spin-glass state.

Model.—In insulating LSCO, holes are trapped by the Coulomb potential of the Sr ions and form hydrogenlike bound states $\psi(\mathbf{r}) = \Psi\chi(\mathbf{r}) = \Psi\sqrt{2/\pi}\kappa e^{-\kappa r}$. The wave function has two components corresponding to up and down sublattices, described by the two-component spinor Ψ (pseudospin). Mixing between the two sublattices, the physical origin of the spiral, is conveniently described by rotations of these pseudospins [13]. We use $\kappa \approx 0.4$ for the inverse localization length [16] and refer to these bound states as impurities. The temperature corresponding to the binding energy is about $T_b \sim 100$ K [13]; hence at $T \ll T_b$ the charge degrees of freedom are frozen. For even lower temperatures $T \ll T_p \sim 30$ K [14], the orthorhombic distortion pins the impurities to the hole pocket centered on the b axis, which according to Ref. [13] induces spirals directed along the b direction. Since we consider $T \ll T_p$, the relevant degrees of freedom are the spins of the Cu ions and the impurity pseudospins.

In the framework of the nonlinear σ model (NLSM), the staggered component of the copper spins is described by a continuous vector field $\vec{n}(\mathbf{r})$. Using the orthorhombic coordinate system, see Fig. 1, we denote vectors acting in spin space by arrows and chose the bold font for vectors in coordinate space. Having in mind the above discussion of the effective degrees of freedom, we write the energy of a single layer of LSCO as

$$\frac{\rho_s}{2}\int d^2r\left\{[\nabla\vec{n}(\mathbf{r})]^2 + \frac{D^2}{c^2}[n^a(\mathbf{r})]^2 + \frac{\Gamma_c}{c^2}[n^c(\mathbf{r})]^2\right\} + 2\sqrt{2}g\sum_i\int d^2r\rho(\mathbf{r}-\mathbf{r_i})[\vec{n}(\mathbf{r})\times\vec{l}_i](\mathbf{e}_b\cdot\nabla)\vec{n}(\mathbf{r}), \quad (1)$$

where n^α, $\alpha = a, b, c$, denotes the components of the $\vec{n}$ field, subject to the constraint $\vec{n}^2 = 1$. The first line in Eq. (1) is the elastic energy [17] which takes into account the Dzyaloshinski-Moriya (DM) and the XY anisotropies,

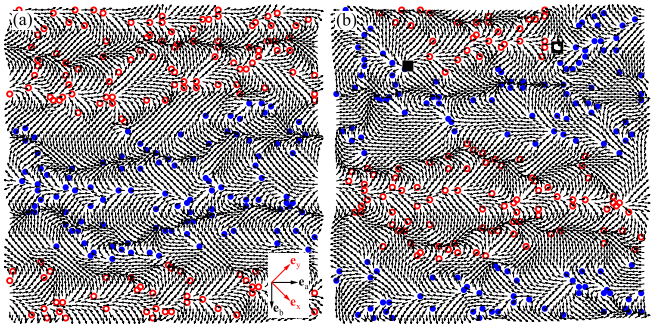

FIG. 1 (color online). Characteristic ground state configuration of a particular realization at $x = 0.05$. The system (a) without defects has higher energy than the same system (b) with a vortex-antivortex pair (squares). The impurity pseudospins l_i are oriented along the c axis. Full (open) circles correspond to values $-\frac{1}{2}$ ($+\frac{1}{2}$). Small arrows represent the $\vec{n}$ field. The system forms domains stretched along the a direction, in which all pseudospins are aligned in parallel.

with $D \approx 2.5$ meV and $\sqrt{\Gamma_c} \approx 5$ meV. These parameters follow from neutron scattering data at zero doping [18]. We use $\rho_s \approx 0.18J$ for the spin stiffness and $c \approx 1.66J$ for the spin-wave velocity, with $J \approx 130$ meV. The second line in Eq. (1) represents the interaction of the $\vec{n}$ field with the impurity pseudospins $\vec{l}_i = \frac{1}{2}\Psi_i^\dagger \vec{\sigma} \Psi_i$; see Ref. [14]. The impurities are located at positions $\mathbf{r}_i$ and $\rho(\mathbf{r}) = \chi^2(\mathbf{r})$. The coupling constant $g \approx J$ has been calculated previously within the extended t-J model [12]. Equation (1) describes the static limit of the effective field theory. This limit is sufficient to study ground state properties because (1) results in a long-range interaction [see Eq. (4) below].

The anisotropies in Eq. (1) pin the $\vec{n}$ field to a particular spatial direction. Because the XY term is larger than the DM anisotropy, $\sqrt{\Gamma_c} > D$, the staggered field $\vec{n}$ is coplanar and lies in the ab plane [19]. For a single CuO_2 layer at zero temperature, there is no mechanism that deflects $\vec{n}$ out of this plane. Substituting $\vec{n} = (n^a, n^b, n^c) = (\sin\theta, \cos\theta, 0)$ in Eq. (1), the energy of the effective $O(2)$ NLSM reads

$$\frac{\rho_s}{2} \int d^2r \Big\{ [\nabla\theta(\mathbf{r})]^2 + 4\mathcal{M} \sum_i l_i \rho(\mathbf{r} - \mathbf{r}_i)(\mathbf{e}_b \cdot \nabla)\theta(\mathbf{r}) \Big\}, \tag{2}$$

where $l_i = \frac{1}{2}\Psi_i^\dagger \sigma^c \Psi_i$ is an Ising variable taking the values $\pm\frac{1}{2}$ and $\mathcal{M} = \sqrt{2}g/\rho_s \approx 8$. In Eq. (2), we have neglected the DM term $D^2/c^2 \sin^2\theta$ because in the spin-glass phase, the angle $\theta(\mathbf{r})$ quickly varies at a scale much shorter than $l_{DM} = c/D \sim 100$ and since $\langle \sin^2\theta \rangle = \frac{1}{2}$, the DM term can be safely neglected. We thus assume that the only effect of the DM term is to pin the direction of the staggered magnetization in the Néel phase. Very importantly, Eq. (2) is exact in the sense that it is valid for arbitrary θ and not restricted to small angles.

To integrate out the θ field, we start with a single impurity. The variation of Eq. (2) with respect to θ yields $-\nabla^2\theta(\mathbf{r}) + 2\mathcal{M} l (\mathbf{e}_b \cdot \nabla)\rho(\mathbf{r}) = 0$, which has the solution $\theta(\mathbf{r}) = l\vartheta(\mathbf{r})$, where $\vartheta(\mathbf{r}) = \frac{\mathcal{M}}{\pi} \frac{\mathbf{e}_b \cdot \mathbf{r}}{r^2} \{(1 + 2\kappa r)e^{-2\kappa r} - 1\}$. Because of the linearity of the problem, the solution for N impurities is the superposition

$$\theta(\mathbf{r}) = \sum_{i=1}^{N} l_i \vartheta(\mathbf{r} - \mathbf{r}_i). \tag{3}$$

Substituting this solution into Eq. (2) yields an expression of the energy in terms of the Ising pseudospins l_i only

$$E_I = \frac{2\rho_s \mathcal{M}^2 \kappa^2}{\pi} \sum_{i \neq j}^{N} l_i l_j \{F_1(\kappa r_{ij}) + \cos(2\alpha_{ij}) F_2(\kappa r_{ij})\}, \tag{4}$$

with $F_1(y) = -y^2 K_2(2y)$ and $F_2(y) = 1/y^2 - yK_3(2y) - y^2 K_2(2y)$. Here α_{ij} is the angle between the vectors $\mathbf{e}_b$ and $\mathbf{r}_{ij} = \mathbf{r}_i - \mathbf{r}_j$, and K_n are modified Bessel functions. For $r \gg 1/\kappa$, the above expression is equivalent to the usual dipole-dipole interaction [$\propto \cos(2\alpha_{ij})/r_{ij}^2$].

Ground state and destruction of Néel order.—We perform classical Monte Carlo simulation to find the ground state of the Ising pseudospins described by Eq. (4) using the same algorithm as in Ref. [14]. We average observables over many realizations of random impurity distributions. For a particular realization, we consider up to $N = 200$ Ising pseudospins l_i on a square lattice of size $L = \sqrt{N/x}$. In order to minimize finite-size effects, we orient the lattice along the orthorhombic coordinate system, apply periodic boundary conditions along the a axis and extract relevant quantities only from the central quarter of the system. The b direction is left open, in order not to impose an artificial constraint on the spiral pitch. Once the Ising ground state is found, the $\vec{n}$ field is determined according to Eq. (3). Note that $\theta(\mathbf{r})$ in (3) can always be shifted by a constant θ_0. We set $\theta_0 = 0$ and therefore have $\theta = 0$ and $\vec{n} = \vec{e}_b$ in the undoped system. Figure 1(a) shows a characteristic ground state for a particular realization at doping $x = 0.05$. The systems forms large domains, stretched along the a axis, in which all pseudospins point in the same direction. The presence of Néel order can be identified as a nonzero $\langle n^b \rangle$. For a given doping, the average is taken over the central quarter of the system and over many realizations of random impurity positions. We first performed calculations for $\kappa \to \infty$ (pointlike impurities) and found that Néel order is not destroyed at least up to $x = 0.05$; see Fig. 2(a). In this case, the pseudospins align in an antiparallel pattern along the b direction, on a scale of the order of the separation between impurities. The angle θ is thus small and the resulting n field never completes a full rotation. For finite κ, the situation is qualitatively different because for sufficiently small distances between impurities, the combination in brackets $\{\ldots\}$ in Eq. (4) is always negative. This

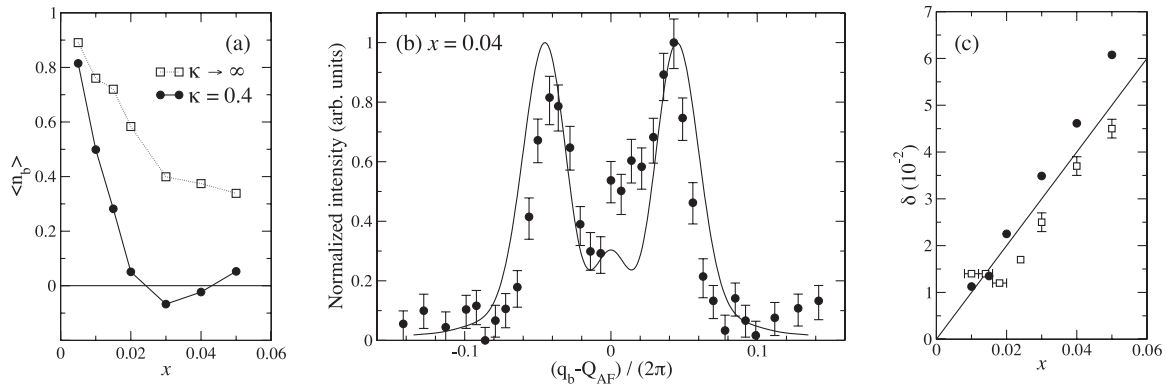

FIG. 2. (a) $\langle n^b \rangle$ as a function of doping x. For $\kappa = 0.4$, Néel order is destroyed at $x_c \approx 0.02$, in agreement with experiments. For pointlike impurities ($\kappa \to \infty$), there is no phase transition at least up to $x = 0.05$. (b) Neutron scattering probability $S_{\mathbf{q}}$ for $x = 0.04$. Dots correspond to experimental observations taken from Fig. 4 in Ref. [6], with normalized intensities. The curve represents our simulation, containing no fitting parameters. (c) Incommensurability δ (in reciprocal lattice units of the tetragonal lattice) as a function of doping. Our calculations (dots) are in good agreement with experimental measurements (squares) taken from Ref. [3,5,24], see Fig. 6 of Ref. [3]. Theoretical points for the Néel phase are taken from Ref. [14].

favors parallel alignment of the pseudospins and hence leads to the formation of parallel Ising domains; see Fig. 1(a). The domains have a finite width because the long-range tail of Eq. (4) still favors antiparallel alignment along the b direction. The width w depends on doping and on κ, but also on the size of the lattice as $w \propto \sqrt{L}$. The domains thus become macroscopic in the thermodynamic limit. The mechanism for the domain formation is exactly the same as for ferromagnets [20]. We will show that topological defects lead to finite, but still very large domain sizes. The doping dependence of $\langle n^b \rangle$ for $\kappa = 0.4$ is shown in Fig. 2(a). The phase transition takes place at $x_c \approx 0.02$, in very good agreement with experiments. The small deviations from zero at $x \geq 0.02$ in Fig. 2(a) are due to finite-size effects. It is remarkable that the correct critical concentration x_c is obtained for $\kappa \approx 0.4$ that is known from the variable range hopping conductivity [16].

Topological defects.—There are two kinds of topological defects in a 2D $O(3)$ NLSM, vortices and instantons [21]. Instantons lead to noncoplanar spin configurations that, according to our calculations, increase the energy because the system prefers coplanar pseudospin arrangements. Instantons are therefore not present in the ground state. For vortices, the situation is different. Let us consider solutions of the Laplace equation $\nabla^2 \theta = 0$ of the form $\theta_v(\mathbf{r}) = \sum_{j=1}^{M} Q_j \arg[x - X_j + i(y - Y_j)]$. Here $\mathbf{R}_j = (X_j, Y_j)$ and $Q_j \in \mathbb{Z}$ are the positions of the defects and their topological charges (winding numbers), respectively. The energy is minimal for vanishing total topological charge with $Q_j = \pm 1$. In this case, we have $M/2$ pairs of vortices with opposite winding numbers. For large average separation between vortices, $R \gg 1$, the associated energy calculated with logarithmic accuracy is [21]

$$E_V = M \pi \rho_s \ln R. \tag{5}$$

Because this energy is positive, vortices never appear in the ground state of the NLSM without impurities. However, in a doped system, one also has to take into account the interaction energy E_{IV} between impurities and vortices. From Eq. (2), we find

$$E_{IV} = 2\rho_s \mathcal{M} \sum_{i,j=1}^{N,M} l_i Q_j \frac{\mathbf{e}_a \cdot \boldsymbol{\xi}_{ij}}{\xi_{ij}^2} [1 - e^{-2\kappa \xi_{ij}} (1 + 2\kappa \xi_{ij})], \tag{6}$$

where $\boldsymbol{\xi}_{ij} = (\mathbf{R_j} - \mathbf{r_i})$ are the positions of the vortices with respect to the impurities. The interaction energy (6) is large and negative because of the domains formed in the spin-glass phase in which all pseudospins point in the same direction. It therefore favors the creation of vortices at zero temperature. The total energy is now given by the sum of Eqs. (4)–(6). An illustration of a system with one vortex-antivortex pair is shown in Fig. 1(b). Compared to the same realization without defects [Fig. 1(a)], the energy is around 10% lower. The presence of vortices renders the problem of finding the ground state quite difficult. In addition to minimizing the energy of the Ising pseudospins, one also has to check if vortex-antivortex pairs can lower the energy, and if so, optimize their positions. Nevertheless, it is possible to estimate the optimal distance between defects in the thermodynamic limit. Because of the long-range nature of the interaction (6), the energy gain is proportional to R. Let us denote the energy of the system without vortices by $E = E_I$ and use $\tilde{E} = \tilde{E}_I + E_{IV} + E_V$ for a system with M defects. The energy gain due to vortices can then be expressed as $\Delta E = \tilde{E} - E = -\gamma x M R + M \pi \rho_s \ln R$. By comparing the energies of systems with 4 and 16 vortices to the same realizations without defects, we find that the parameter γ is weakly doping dependent. At $x = 0.02$, we obtain $\gamma \approx 2.0$, leading to an optimal distance $R_{\text{opt}} \approx 130$ in the thermodynamic limit and at

$x = 0.05$, we find $\gamma \approx 1.1$ from which we deduce $R_{\text{opt}} \approx 90$. We thus conclude that vortex-antivortex pairs break up the domains and lead to a parquetlike arrangement of Ising pseudospins with a natural domain size $R \approx 100$.

Interestingly, there is no irreversible glassy behavior in this spiral state. Although one could think that glassiness is due to the long-range character of the interaction, we have checked that changing the boundary conditions or the size of the system only has a marginal influence on the energy. In principle, the irreversibility could also arise from topological defects; however, this is unlikely because of their very high energy. The state we have found is therefore not a proper glass and we believe that the commonly used ''spin-glass'' term does not reflect the most important properties of this state. This claim is supported by experimental observations: While the incommensurate structure is already observed below 30–40 K, the irreversible glassy behavior only sets in below $T \sim 5$–6 K [22] and is in our opinion due to the interlayer interaction that leads to a freezing of incompatible spiral configurations in neighboring planes.

Static spin structure factor and neutron scattering.—Let us finally calculate the structure factor $S_{\mathbf{q}} = \frac{1}{L^2}\sum_{ij,\alpha} e^{i\mathbf{q}\cdot(\mathbf{r}_i-\mathbf{r}_j)} n^{\alpha}(\mathbf{r}_i) n^{\alpha}(\mathbf{r}_j)$, which is related to the neutron scattering cross section. Figure 2(b) shows experimental data taken by Fujita *et al.* [6] on a sample with doping $x = 0.04$ together with our theoretical results for $S_{\mathbf{q}}$. The agreement between theory and experiment is quite remarkable, especially given the fact that it is not restricted to a particular sample, but can be observed over a broad range of doping. This latter finding is illustrated in Fig. 2(c), which shows the incommensurability δ, defined as half the distance between the peaks, as a function of doping. Expressed in reciprocal lattice units of the tetragonal structure, the incommensurability is in good approximation proportional to doping, $\delta \approx x$. Because of their low density, topological defects do not have a major influence on $S_{\mathbf{q}}$ and only lead to some broadening of the peaks.

To conclude, we have developed the effective low-energy field theory that describes the magnetic structure of $La_{2-x}Sr_xCuO_4$ in the spin-glass phase ($x \lesssim 0.055$). We have shown that the staggered component of the copper spins is confined to the ab plane, due to the XY anisotropy. The static spin structure factors obtained in our approach are in excellent agreement with neutron scattering data, over a whole range of doping. We have analyzed the transition from the Néel to the spin-glass phase, which is similar to that of a ''Lifshitz point'' separating two magnetically ordered phases [11,23] and we have shown that topological defects (spin vortices) play a significant role in the ground state of the spin-glass phase.

We would like to thank A. N. Lavrov for valuable discussions. A. I. M. gratefully acknowledges the School of Physics at the University of New South Wales for warm hospitality and financial support during his visit. The Monte Carlo simulations have been performed on computers belonging to the Institut Romand de Recherche Numérique en Physique des Matériaux (IRRMA) in Switzerland.

[1] B. Keimer *et al.*, Phys. Rev. B **45**, 7430 (1992).
[2] M. A. Kastner *et al.*, Rev. Mod. Phys. **70**, 897 (1998).
[3] M. Matsuda *et al.*, Phys. Rev. B **65**, 134515 (2002).
[4] S. Wakimoto *et al.*, Phys. Rev. B **60**, R769 (1999).
[5] M. Matsuda *et al.*, Phys. Rev. B **62**, 9148 (2000).
[6] M. Fujita *et al.*, Phys. Rev. B **65**, 064505 (2002).
[7] K. Yamada *et al.*, Phys. Rev. B **57**, 6165 (1998).
[8] N. Hasselmann, A. H. Castro Neto, and C. Morais Smith, Phys. Rev. B **69**, 014424 (2004).
[9] V. Juricic *et al.*, Phys. Rev. Lett. **92**, 137202 (2004).
[10] P.-A. Lindgård, Phys. Rev. Lett. **95**, 217001 (2005).
[11] V. Juricic, M. B. Silva-Neto, and C. Morais Smith, Phys. Rev. Lett. **96**, 077004 (2006).
[12] O. P. Sushkov and V. N. Kotov, Phys. Rev. B **70**, 024503 (2004).
[13] O. P. Sushkov and V. N. Kotov, Phys. Rev. Lett. **94**, 097005 (2005).
[14] A. Lüscher *et al.*, Phys. Rev. B **73**, 085122 (2006).
[15] B. I. Shraiman and E. D. Siggia, Phys. Rev. Lett. **62**, 1564 (1989).
[16] C. Y. Chen *et al.*, Phys. Rev. B **51**, 3671 (1995).
[17] J. Chovan and N. Papanicolaou, Eur. Phys. J. B **17**, 581 (2000); M. B. Silva Neto and L. Benfatto, Phys. Rev. B **72**, 140401(R) (2005).
[18] B. Keimer *et al.*, Z. Phys. B **91**, 373 (1993).
[19] If $\sqrt{\Gamma_c} < D$, the $\vec{n}$ field is confined in the bc plane.
[20] See, e.g., C. Kittel, *Introduction to Solid State Physics* (Wiley, New York, 1995), 7th ed.
[21] See, e.g., A. M. Polyakov, *Gauge Fields and Strings* (Harwood Academic Publishers, Chur, 1987).
[22] Ch. Niedermayer *et al.*, Phys. Rev. Lett. **80**, 3843 (1998); S. Wakimoto *et al.*, Phys. Rev. B **62**, 3547 (2000).
[23] L. Capriotti and S. Sachdev, Phys. Rev. Lett. **93**, 257206 (2004).
[24] S. Wakimoto *et al.*, Phys. Rev. B **61**, 3699 (2000).